

The following resources related to this article are available online at www.sciencemag.org (this information is current as of December 4, 2009):

Updated information and services, including high-resolution figures, can be found in the online version of this article at:

<http://www.sciencemag.org/cgi/content/full/310/5756/1957>

Supporting Online Material can be found at:

<http://www.sciencemag.org/cgi/content/full/310/5756/1957/DC1>

A list of selected additional articles on the Science Web sites **related to this article** can be found at:

<http://www.sciencemag.org/cgi/content/full/310/5756/1957#related-content>

This article **cites 17 articles**, 6 of which can be accessed for free:

<http://www.sciencemag.org/cgi/content/full/310/5756/1957#otherarticles>

This article has been **cited by** 47 article(s) on the ISI Web of Science.

This article has been **cited by** 14 articles hosted by HighWire Press; see:

<http://www.sciencemag.org/cgi/content/full/310/5756/1957#otherarticles>

This article appears in the following **subject collections**:

Development

<http://www.sciencemag.org/cgi/collection/development>

Information about obtaining **reprints** of this article or about obtaining **permission to reproduce this article** in whole or in part can be found at:

<http://www.sciencemag.org/about/permissions.dtl>

In key *C. elegans* adult tissues, the *lin-4* miRNA may act to suppress the translation of *lin-14*, preventing *lin-14* from affecting the transcription of a yet unidentified factor that regulates or interacts with the *daf-2* insulin/IGF-1 pathway. By demonstrating that *lin-4* and *lin-14*, two key temporal regulators of development, also influence the rate of aging, we provide support for the theory that life span is affected by an innate, programmed timing mechanism. However, our data are also consistent with an alternative theory of aging, antagonistic pleiotropy, which posits that genes with primary roles in development can later secondarily influence life span (27). miRNAs are important regulators of development, apoptosis, and metabolism (28–31), and our work demonstrates that a miRNA can regulate aging, possibly through the insulin-like signaling pathway. It is possible that the mammalian *lin-4* miRNA homologs, the *miR-125* family, may regulate processes responsible for life-span determination in vertebrates.

fgf20 Is Essential for Initiating Zebrafish Fin Regeneration

Geoffrey G. Whitehead, Shinji Makino, Ching-Ling Lien, Mark T. Keating*

Epimorphic regeneration requires the presence or creation of pluripotent cells capable of reproducing lost organs. Zebrafish fin regeneration is mediated by the creation of blastema cells. Here, we characterize the *devoid of blastema* (*dob*) mutant that fails fin regeneration during initial steps, forms abnormal regeneration epithelium, and does not form blastema. This mutation has no impact on embryonic survival. *Dob* results from an *fgf20a* null mutation, Y148S. *Fgf20a* is expressed during initiation of fin regeneration at the epithelial-mesenchymal boundary and later overlaps with the blastema marker *msxb*. Thus, *fgf20a* has a regeneration-specific requirement, initiating fin regeneration, and controlling blastema formation.

Vertebrate regeneration is of scientific and medical interest. Although acute tissue regeneration in humans is limited, other vertebrates possess extraordinary regenerative capabilities. Zebrafish are amenable to genetic analyses and regenerate an impressive array of structures, including spinal cord, optic nerve, heart, and fins (1–3). Zebrafish fin regeneration is marked by five stages: regeneration epithelialization, mesenchymal disorganization, blastema formation, regenerative outgrowth, and termination. Although genetic analyses have enhanced our understanding of fin regeneration (1, 4–6), the

References and Notes

- C. Kenyon, *Cell* **120**, 449 (2005).
- S. A. McCarrroll et al., *Nat. Genet.* **36**, 197 (2004).
- C. Kenyon, in *C. elegans II: Monograph* 33, D. L. Riddle, Ed. (Cold Spring Harbor Laboratory, Plainview, New York, 1997), p. xvii, p. 796.
- T. Lu et al., *Nature* **429**, 883 (2004).
- V. Ambros, H. R. Horvitz, *Genes Dev.* **1**, 398 (1987).
- D. Banerjee, F. Slack, *Bioessays* **24**, 119 (2002).
- F. Slack, G. Ruvkun, *Annu. Rev. Genet.* **31**, 611 (1997).
- R. C. Lee, R. L. Feinbaum, V. Ambros, *Cell* **75**, 843 (1993).
- B. Wightman, I. Ha, G. Ruvkun, *Cell* **75**, 855 (1993).
- P. H. Olsen, V. Ambros, *Dev. Biol.* **216**, 671 (1999).
- R. Feinbaum, V. Ambros, *Dev. Biol.* **210**, 87 (1999).
- G. Ruvkun, J. Giusto, *Nature* **338**, 313 (1989).
- Y. Hong, R. C. Lee, V. Ambros, *Mol. Cell. Biol.* **20**, 2285 (2000).
- L. P. Lim et al., *Genes Dev.* **17**, 991 (2003).
- A. Esquela-Kerscher et al., *Dev. Dyn.* **234**, 868 (2005).
- B. Wightman, T. R. Burglin, J. Gatto, P. Arasu, G. Ruvkun, *Genes Dev.* **5**, 1813 (1991).
- D. Garigan et al., *Genetics* **161**, 1101 (2002).
- C. Kenyon, J. Chang, E. Gensch, A. Rudner, R. Tabtiang, *Nature* **366**, 461 (1993).
- K. Lin, J. B. Dorman, A. Rodan, C. Kenyon, *Science* **278**, 1319 (1997).
- P. L. Larsen, P. S. Albert, D. L. Riddle, *Genetics* **139**, 1567 (1995).
- K. D. Kimura, H. A. Tissenbaum, Y. Liu, G. Ruvkun, *Science* **277**, 942 (1997).
- G. J. Lithgow, T. M. White, S. Melov, T. E. Johnson, *Proc. Natl. Acad. Sci. U.S.A.* **92**, 7540 (1995).
- S. S. Lee et al., *Nat. Genet.* **33**, 40 (2003).
- S. Ogg et al., *Nature* **389**, 994 (1997).
- A. L. Hsu, C. T. Murphy, C. Kenyon, *Science* **300**, 1142 (2003).
- K. Lin, H. Hsin, N. Libina, C. Kenyon, *Nat. Genet.* **28**, 139 (2001).
- K. A. Hughes, R. M. Reynolds, *Annu. Rev. Entomol.* **50**, 421 (2005).
- D. P. Bartel, *Cell* **116**, 281 (2004).
- J. Brennecke, D. R. Hipfner, A. Stark, R. B. Russell, S. M. Cohen, *Cell* **113**, 25 (2003).
- M. N. Poy et al., *Nature* **432**, 226 (2004).
- B. J. Reinhart et al., *Nature* **403**, 901 (2000).
- We thank A. Esquela-Kerscher, D. Banerjee, and K. Carter for critical reading of this manuscript; K. Carter and L. Bai for providing the *zals1* strain; S. S. Lee for technical advice; and R. Lee and V. Ambros, and the *C. elegans* Genetic Center, for supplying strains. This work was supported by an NIH grant (GM64701) to F.S.

Supporting Online Material

www.sciencemag.org/cgi/content/full/310/5756/1954/DC1

Materials and Methods

Figs. S1 to S4

Table S1

References and Notes

1 June 2005; accepted 10 November 2005

10.1126/science.1115596

We expected that *dob* would also disrupt embryogenesis (1, 4–6). However, at 33°C, *dob* viability was comparable with wild type (fig. S1A). Half (23/46) of *dob* adults developed asymmetric caudal fin lobes when heat-shocked as embryos, yet all wild type (41/41) developed symmetric fin lobes (fig. S1B). The total size of wild-type and *dob* caudal fins was comparable (fig. S1B). Therefore, there appears to be an incompletely penetrant ts patterning defect in *dob* (8). Survival of *dob* adults at 33°C was also comparable to wild type (fig. S1C). These data suggest a regeneration-specific requirement for *dob*.

To determine the cellular nature of *dob* regenerative failure, we examined histology of regenerates at 33°C. The first stage of regeneration, formation of regeneration epithelium, appeared abnormal. At 6 and 12 hours post-amputation (*hpa*), *dob* regenerates demonstrated a thickened regeneration epithelium (Fig. 2A). Epithelial proliferation levels in *dob* at 6 and 12 *hpa* were similar to wild type (fig. S3A). Therefore, thickened regeneration epithelium likely results from aberrant epithelial migration (9, 10).

To determine whether *dob* resulted from a primary defect in wound healing, we performed a longitudinal incision along the caudal fin and allowed healing at 33°C. The wild-type response to this injury is nonregenerative, as the wound is covered by epithelium and leaves a slit down the fin. We found no difference in the timing, histochemistry, or bromodeoxyuridine (BrdU) immunohistochemistry of wound-healing between wild type and *dob* (fig. S3B). The possibility remains that the *dob* mutant may have a subtle defect in wound-healing not identified by our observations.

Howard Hughes Medical Institute, Department of Cell Biology, Harvard Medical School, Department of Cardiology, Children's Hospital, Boston, MA 02115, USA.

*To whom correspondence should be addressed. E-mail: mark.keating@novartis.com

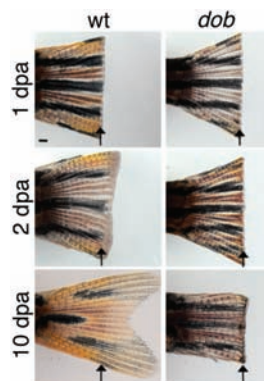


Fig. 1. *dob*, a mutant with early fin regeneration block. Regenerating wild-type (wt) and *dob* fins at 33°C following amputation. Arrows mark amputation plane. At 1 dpa, both wt and *dob* have covered the amputation with epithelium. By 2 dpa, wt fins have regenerated beyond the amputation plane, whereas *dob* mutants have not. At 10 dpa, wt has undergone full reconstitution, but *dob* fails to regenerate. Scale bars, 400 μ m.

To further characterize the *dob* defect in regeneration epithelialization, we performed in situ hybridization experiments. The wild-type regeneration epithelium at 24 hpa is molecularly and histochemically distinct. Specifically, the basal epithelium in wild-type regenerates consists of ordered linear cuboidal epithelial cells (11). In *dob*, the basal epithelium lacked the distinctive cuboidal shape and was non-linear. *Lef1*, a transcription factor downstream of Wnt (12), and *sparc*, a matricellular protein (13), both demarcate regeneration basal epithelium. *Lef1* and *sparc* in situ hybridization in *dob* revealed absent basal epithelial expression (Fig. 2B). Thus, normal formation of a basal regeneration epithelium appears essential for fin regeneration.

At 18 hpa in wild-type regenerates, disorganized mesenchymal cells beneath the amputation plane are considered evidence of dedifferentiation (9, 11). *dob* mutants did not undergo mesenchymal disorganization (Fig. 2A). In 18 hpa wild-type regenerates, *hsp60* is up-regulated in mesenchymal cells destined to form blastema (6). However, *dob* did not express *hsp60* in these cells (fig. S2B). These data suggest a mesenchymal disorganization defect in *dob*.

Mesenchymal disorganization is followed by cell proliferation, migration, and blastema formation (9, 10). The blastema is a mass of undifferentiated mesenchymal cells that have proliferated beyond the amputation plane to drive fin regrowth. At 36 hpa, wild-type regenerates show proper blastema formation; however, *dob* is devoid of blastema (Fig. 2A). These data indicate that *dob* does not initiate fin regeneration and fails to form regeneration epithelium and blastema.

To determine the effect of *dob* on blastema formation, we performed in situ hybridization

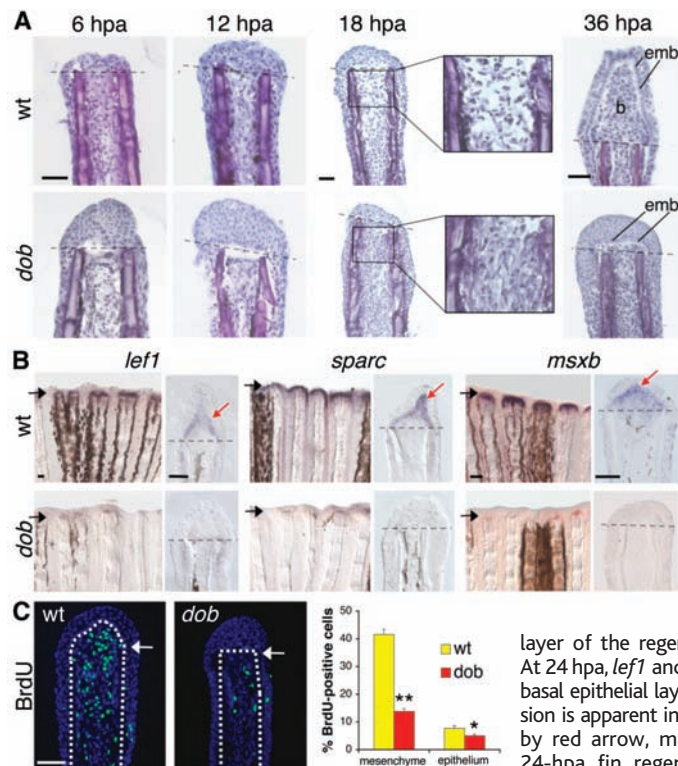


Fig. 2. *dob* fails to initiate fin regeneration and does not form a blastema. Dashed line or arrow marks amputation plane. (A) Hematoxylin-stained sections of caudal fin regenerates. At 6 and 12 hpa, the regeneration epithelium in *dob* is thicker than wild type (wt). At 18 hpa, the regeneration epithelium in *dob* is thicker than wild type (wt). At 18 hpa, the regeneration epithelium is apparent in wt fins but was not observed in *dob*. At 36 hpa, a blastema is seen in wt regenerates, yet *dob* lacks blastema. b, blastema; emb, epithelial-mesenchymal boundary. (B) *lef1* and *sparc* mark the basal epidermal layer of the regeneration epithelium in wt. At 24 hpa, *lef1* and *sparc* are absent from the basal epithelial layer in *dob*. No *msxb* expression is apparent in *dob*. Violet stain, indicated by red arrow, marks gene expression. (C) 24-hpa fin regenerates stained for BrdU (green) and 4',6'-diamidino-2-phenylindole (blue). White dashed line marks epithelial-mesenchymal boundary. During blastema formation, mutants had reduced mesenchymal and epithelial proliferation ($n = 19$). Graph displays the indices of proliferation in mesenchyme and epithelium of wt and *dob* regenerates. **, $P < 0.01$; *, $P < 0.05$. Scale bars, 50 μ m (A), 100 μ m [(B) and (C)].

experiments. In 24 hpa wild-type fins, *msxb* marks rudimentary blastema cells, the mesenchyme distal to the amputation plane. At 72 hpa, during regenerative outgrowth, *msxb* marks distal blastema (7, 9). No *msxb* expression was apparent in *dob* at 24 hpa during blastema formation (Fig. 2B). Faint *msxb* expression was present in *dob* at 72 hpa at the central tip of mesenchyme (fig. S2C). These *msxb*-positive cells may represent a later, inadequate attempt at blastema formation. These data demonstrate that *dob* lacks early *msxb* expression and does not form blastema.

During blastema formation, mesenchymal cells reenter the cell cycle and begin to proliferate (9, 10). These cells migrate toward regeneration epidermis and form the rudimentary blastema. To further define the mechanism of the *dob* regenerative defect, we examined DNA replication, through BrdU labeling. At 24 hpa, *dob* mesenchymal proliferation levels were one-third of wild type, and epithelial proliferation was slightly lower (Fig. 2C). These data indicate that *dob* fails to form a blastema through an early defect in mesenchymal proliferation.

To identify the *dob* gene, we raised 2027 zebrafish from *dob*^{-/-} \times *dob*^{+/-} mapping crosses to adulthood at 25°C, scored for regenerative defects at 33°C, and genotyped these animals (1, 4–6). Two markers, *bet7* and *tof24*, flanked

the 0.2 centimorgan (cM) *dob* critical region on chromosome 1. *fgf20a* was the only transcript within this region, genetically excluding neighboring transcripts (Fig. 3A). Syntenic multicontig alignments demonstrated that no transcripts were located between *efha2* and *fgf20a* in human or fugu databases.

To identify the *dob* mutation, we performed DNA sequence analysis of *fgf20a*. We discovered one missense mutation, an adenine-443 to cytosine (A443C) transversion, in the *fgf20a* gene of *dob* that converted tyrosine-148 to serine (Y148S) (Fig. 3B). We genotyped 140 *dob* mutants, 30 *dob* heterozygotes, and 20 wild-type controls and verified that the A443C transversion cosegregated with the *dob* phenotype. *dob* was isolated in the SJD background, and DNA sequence of *fgf20a* in wild-type SJD revealed no mutation. Therefore, the A443C transversion in *dob* was caused by ENU mutagenesis. This point mutation was not found among five commonly used laboratory strains, indicating that A443C is not a polymorphism. These data indicate that the *dob* phenotype results from *fgf20a* Y148S.

Fgf20 is a newly identified member of the Fgf family. Fgf20 is overexpressed in cancer cell lines, promotes proliferation and differentiation of myocardial cells, and enhances survival of dopaminergic neurons in the adult brain, functions consistent with a role in regeneration (14–16). Y148 exists in the highly

Fig. 3. *fgf20a* Y148S missense mutation causes *dob*. (A) Genetic map of *dob* on chromosome 1. Refined linkage analysis mapped *dob* to the 0.2 cM region between *bef7* and *tof24*. The only gene between flanking recombinant markers is *fgf20a*. Numbers above linear map quantify recombination events between *dob* and linked markers from 2027 meioses. *Bef7*, *fe12*, *mt254*, *tof24*, and *et6* are polymorphic genetic markers between AB and SJD strains identified by random DNA amplification and sequencing within the *dob* critical region. (B) DNA sequence chromatograms of wild-type, *dob*^{+/-}, and *dob*^{-/-} fish. A443C transversion leads to Y148S amino acid substitution. (C) Tyr-148 is conserved across vertebrates and among most zebrafish Fgfs. (D) Fgf secondary β -trefoil structure. Tyr-148 is located in the $\beta 9$ strand of Fgf20a. (E) Phenotypic classes and frequencies (%) obtained after injection of wild-type *fgf20a*, Y148S *fgf20a*, wild-type *fgf3*, or Y148C *fgf3* mRNAs (10 ng/ μ l) into wild-type embryos. Y148S *fgf20a* had no effect on the embryo, suggesting loss of function. Wt, normal; p1, head reduction, loss of tail; p2, lysis.

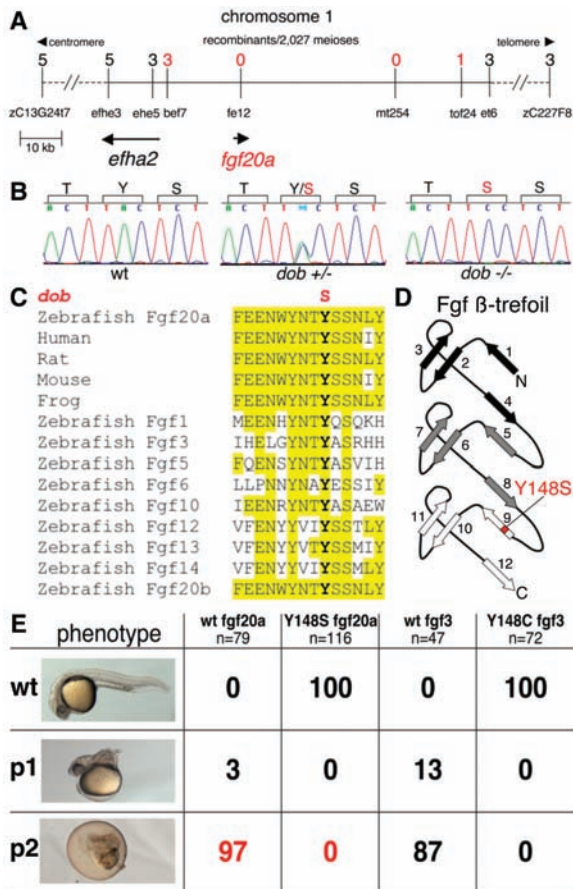
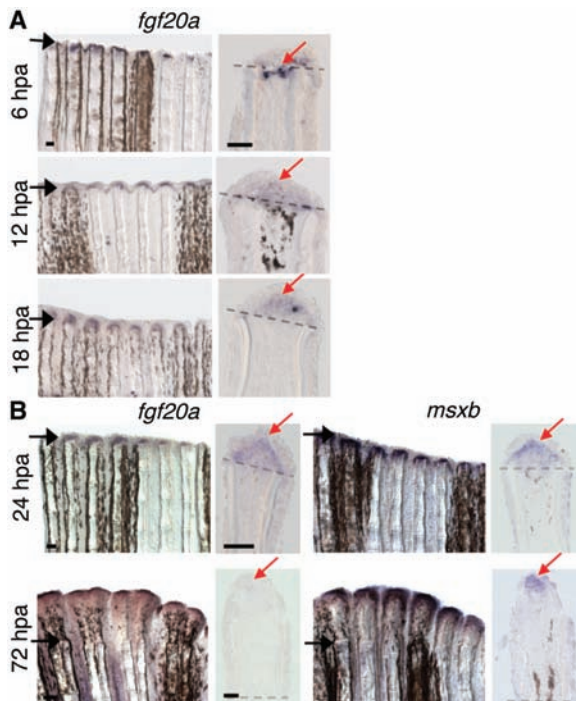


Fig. 4. *fgf20a* expression localizes to epithelial-mesenchymal boundary during initiation of fin regeneration. (A) Whole-mount in situ hybridization and sections showing *fgf20a* expression. During initiation of fin regeneration (6 to 12 hpa), *fgf20a* expression is localized to mesenchymal cells directly underneath the regeneration epithelium. During early blastema formation (18 hpa), *fgf20a* is confined to the blastema. (B) During blastema formation (24 hpa), *fgf20a* and *msxb* colocalize in blastema cells. *fgf20a* and *msxb* expression domains overlap at 72 hpa, when *fgf20a* is concentrated at the distal tip of *msxb*-positive distal blastema. Violet stain indicated by red arrow marks expression. Scale bars, 100 μ m.



conserved Fgf-core domain in the $\beta 9$ strand of the 12-strand β -trefoil, adjacent to residues (WYN) (Fig. 3, C and D) that make essential Fgf receptor contacts (17). Y148 is invariant

across vertebrate species of Fgf20 and most zebrafish Fgfs (Fig. 3C). Thus, Y148 is evolutionarily conserved among species and within the Fgf family.

To determine the effect of Y148S on the activity of Fgf20a protein, we carried out over-expression studies in zebrafish embryos. Injection of wild-type *fgf* mRNA leads to dorsalization of the embryo and death (18). Injected *fgf20a* Y148S mRNA failed to recapitulate this phenotype (Fig. 3E). Similar results have been demonstrated for the null *fgf3*²¹¹⁴² allele, a Y148C mutation, the same tyrosine mutated in *dob* (18). These data indicate that Y148S is likely a null mutation and that Y148 is crucial for Fgf function.

To ensure that *fgf20a* Y148S is responsible for the *dob* phenotype, we injected wild-type and *dob* embryos with wild-type *fgf20a* mRNA. We found that 87.8% of wild-type embryos showed dorsalization and lethality, compared with 53.5% of *dob* embryos ($P = 0.02$) (table S1). These data support the view that the *dob* phenotype results from reduced *fgf20a* and that *fgf20a* Y148S causes *dob*.

To define the timing and pattern of *fgf20a* expression during fin regeneration, we performed reverse transcriptase polymerase chain reaction and in situ hybridization experiments. *fgf20a* was expressed as early as 1 hpa. Expression peaked at 6 hpa, gradually declined, peaked again at 24 hpa, then declined (fig. S2D). During initiation of fin regeneration (6 to 12 hpa), *fgf20a* expression was localized to mesenchyme at the epithelial-mesenchymal boundary (Fig. 4A). *fgf20a* was later expressed in blastema during early blastema formation (18 hpa) (Fig. 4A). These data indicate that *fgf20a* is expressed in key regeneration cells during initiation of fin regeneration, consistent with the *dob* phenotype.

We further characterized the expression of *fgf20a* during fin regeneration and compared *fgf20a* and *msxb* expression. At 24 hpa, *msxb* marks rudimentary blastema cells. *fgf20a* expression colocalized with *msxb* in early blastema cells (Fig. 4B). During regenerative outgrowth, at 72 hpa, *msxb* expression marks stem cell-like distal blastema cells (6, 9). *fgf20a* expression was restricted to a subset of *msxb*-positive distal blastema cells (Fig. 4B). These data indicate that *fgf20a* and *msxb* expression overlap during blastema formation and regenerative outgrowth.

We conclude that the *dob* phenotype is caused by a Y148S mutation in Fgf20a. Data implicating *fgf20a* in *dob* include (i) genetic linkage of *dob* to a 70-kb critical interval on chromosome 1, the presence of *fgf20a* in this interval, and the absence of other transcripts; (ii) the presence of an Fgf20a missense mutation (Y148S) in a completely conserved amino acid linked with the *dob* phenotype ($P = 4.22 \times 10^{-42}$, Fisher's Exact test); (iii) the absence of Y148S in five wild-type strains, indicating that this variant is not a polymorphism; (iv) in situ hybridization showing that *fgf20a* is expressed in mesenchymal cells adjacent to regeneration epithelium as early as

6 hpa; (v) functional studies showing that the Y148S mutation leads to loss of function; (vi) DNA microarray data demonstrating disrupted Fgf signaling in *dob* (fig. S4A and table S2); and (vii) insensitivity of *dob* embryos to wild-type *fgf20a* mRNA overexpression (table S1). Thus, the early regenerative defect observed in *dob* results from Fgf20a dysfunction.

We have genetically identified a specific growth factor, Fgf20a, that is essential for initiating fin regeneration, regeneration epithelialization, and blastema formation. These findings provide a genetic foothold on the early signaling events of regeneration that will enable further identification of key regeneration genes. This information will broaden our understanding of regenerative mechanisms and may enable regenerative medicine.

Protein Synthesis upon Acute Nutrient Restriction Relies on Proteasome Function

Ramunas M. Vabulas* and F. Ulrich Hartl*

The mechanisms that protect mammalian cells against amino acid deprivation are only partially understood. We found that during an acute decrease in external amino acid supply, before up-regulation of the autophagosomal-lysosomal pathway, efficient translation was ensured by proteasomal protein degradation. Amino acids for the synthesis of new proteins were supplied by the degradation of preexisting proteins, whereas nascent and newly formed polypeptides remained largely protected from proteolysis. Proteasome inhibition during nutrient deprivation caused rapid amino acid depletion and marked impairment of translation. Thus, the proteasome plays a crucial role in cell survival after acute disruption of amino acid supply.

Protein biosynthesis in mammalian cells relies on the continuous uptake of essential amino acids from the environment. Acute amino acid restriction can occur in several physiological and pathophysiological conditions, such as after disruption of the trans-placental nutrient supply in neonates or during organ ischemia. Up-regulation of the autophagosomal-lysosomal pathway is known to provide free amino acids for protein synthesis under these nutrient stress conditions through the bulk degradation of cytoplasmic proteins and organelles (1, 2). However, this adaptation requires hours to become fully effective (2, 3), suggesting the existence of constitutive mechanisms that protect cells during short-term fluctuations in amino acid supply. Moreover, certain organs, such as the brain, are inefficient in up-regulating autophag-

References and Notes

1. S. L. Johnson, J. A. Weston, *Genetics* **141**, 1583 (1995).
2. T. Becker, M. F. Wullimann, C. G. Becker, R. R. Bernhardt, M. Schachner, *J. Comp. Neurol.* **377**, 577 (1997).
3. K. D. Poss, L. G. Wilson, M. T. Keating, *Science* **298**, 2188 (2002).
4. A. Nechiporuk, K. D. Poss, S. L. Johnson, M. T. Keating, *Dev. Biol.* **258**, 291 (2003).
5. K. Poss, A. Nechiporuk, A. Hillam, S. L. Johnson, M. T. Keating, *Development* **129**, 5141 (2002).
6. S. Makino et al., *Proc. Natl. Acad. Sci. U.S.A.* **102**, 14599 (2005).
7. M. A. Akimenko, S. L. Johnson, M. Westerfield, M. Ekker, *Development* **121**, 347 (1995).
8. Materials and methods are available as supporting material on Science Online.
9. A. Nechiporuk, M. T. Keating, *Development* **129**, 2607 (2002).
10. G. Poleo, C. W. Brown, L. Laforest, M. A. Akimenko, *Dev. Dyn.* **221**, 380 (2001).
11. K. D. Poss, M. T. Keating, A. Nechiporuk, *Dev. Dyn.* **226**, 202 (2003).

12. K. D. Poss, J. Shen, M. T. Keating, *Dev. Dyn.* **219**, 282 (2000).
13. A. D. Bradshaw, E. H. Sage, *J. Clin. Invest.* **107**, 1049 (2001).
14. M. N. Chamorro et al., *EMBO J.* **24**, 73 (2005).
15. K. J. Lavine et al., *Dev. Cell* **8**, 85 (2005).
16. S. Ohmachi, T. Mikami, M. Konishi, A. Miyake, N. Itoh, *J. Neurosci. Res.* **72**, 436 (2003).
17. A. N. Plotnikov, S. R. Hubbard, J. Schlessinger, M. Mohammadi, *Cell* **101**, 413 (2000).
18. W. Herzog et al., *Development* **131**, 3681 (2004).
19. See supporting online text for acknowledgments.

Supporting Online Material

www.sciencemag.org/cgi/content/full/310/5756/1957/DC1

Materials and Methods

SOM Text

Figs. S1 to S4

Tables S1 and S2

References

19 July 2005; accepted 29 November 2005
10.1126/science.1117637

EGFP accumulated to a low steady-state level in transiently transfected cells, reflecting the equilibrium between its synthesis and degradation. As expected, upon inhibition of protein synthesis with cycloheximide (CHX), Ub-EGFP was degraded within minutes (Fig. 1A). In contrast, the addition of the proteasome inhibitor MG132 caused the virtually immediate accumulation of Ub-EGFP (Fig. 1A). To determine whether proteasome inhibition was complete, we analyzed the combined effect of MG132 and CHX. Inhibition of translation by CHX is known to be very rapid and efficient (10, 11). Thus, if MG132 were to block proteasome function only partially, the arrest of translation would lead to a decrease in Ub-EGFP level due to degradation. The simultaneous addition of CHX and MG132 instantaneously stabilized the Ub-EGFP reporter (Fig. 1A). Similar observations were made with the proteasome inhibitors clasto-lactacystin- β -lactone and epoxomicin (11). Thus, under the conditions chosen proteasome inhibition was immediate and essentially complete.

The effect of proteasome inhibition on translation was analyzed under conditions of acute amino acid restriction. The concentrations of the essential amino acids—leucine, phenylalanine, or methionine—were maintained in the range of normal adult plasma levels (12) or were reduced individually 100-fold to create insufficiency in external supply (13). Newly synthesized proteins were labeled with ^{35}S -methionine (^{35}S -Met), followed by cell lysis in SDS and precipitation of proteins with trichloroacetic acid (TCA). Proteasome inhibition with MG132, clasto-lactacystin- β -lactone or epoxomicin markedly impaired translation within 5 to 10 min, but only when cells were incubated in medium deficient in at least one essential amino acid (leucine or phenylalanine) (Fig. 1, B to D, and fig. S1, A and B). Similar results were obtained when cells were incubated in methionine-deficient medium with ^3H -leucine (^3H -Leu) as the tracer

Department of Cellular Biochemistry, Max Planck Institute of Biochemistry, Am Klopferspitz 18, D-82152 Martinsried, Germany.

*To whom correspondence should be addressed. E-mail: vabulas@biochem.mpg.de (R.M.V.); uhartl@biochem.mpg.de (F.U.H.)